ANL-HEP-PR-75-32
July 1975

DEVELOPMENTS IN THE PHENOMENOLOGY OF TWO-TO-THREE PARTICLE REACTIONS*

Edmond L. Berger

High Energy Physics Division
Argonne National Laboratory
Argonne, Illinois 60439

ABSTRACT

Recent progress in understanding data on two to three particle hadron reactions is described. The use of an s-channel azimuthal angle selection is advocated to identify and separate different exchange mechanisms which contribute to the same final state at low subenergy. Solutions to the neutral Q cross-over problem in the Deck model are discussed, and experimental tests are proposed. Methods are offered for enhancing resonance signals in the presence of a large Deck exchange background. The need for absorptive corrections to the usual Deck model is stressed in the light of new FNAL data on diffractive neutron dissociation and ISR data on proton dissociation. Results of an explicit absorbed pion exchange Deck model calculation are compared with data.

*Work performed under the auspices of the United States Energy Research and Development Administration.

I. INTRODUCTION

Reactions in which two hadrons enter and three emerge are the simplest inelastic processes. The recent history of the phenomenology of 2 to 3 particle hadronic reactions dates to 1967, when papers were published by Chan and collaborators[1] at CERN, by Chew and collaborators[1] in Berkeley, and by Zachariasen and Zweig.[1] Their common approach was an extension of peripheral ideas, which had been useful in $2 \to 2$ reactions, to $2 \to 3$ processes. Amplitudes for $2 \to 3$ reactions were based on doubly peripheral graphs, such as sketched in Fig. 1(b), and were meant to be valid only when subenergies are suitably large. In this strict domain of applicability, practical results were severely limited by lack of data. Most events are concentrated in the part of phase space where at least one subenergy is small.

The next development of importance was the advent of explicit dual models. The five-point function, B_5, turned the low subenergy difficulty into an advantage and fits to data provided some valuable lessons.[2] However, the model was soon recognized to be overly rigid, and it passed quietly into disuse.

For most of the past four years, the study of the simplest inelastic processes, $2 \to 3$, has enjoyed benign neglect by most phenomenologists. Our experimental colleagues have not rested, however. Bubble chamber statistics are now an order of magnitude better than they used to be. Several counter spectrometers have been built, at CERN, Argonne, SLAC, BNL, and FNAL. Excellent data are accumulating over a wide range of momenta, from 4 GeV/c at ANL to the highest ISR energies. There are outstanding physics questions we can investigate, such as the role of $2 \to 3$ unitarity; duality constraints in exclusive final states, given an exotic initial state; the relationship of $2 \to 2$ to $2 \to 3$, and of $2 \to 3$ to $2 \to X$; resonance-background

interferences; the phase structure of the two-Reggeon one-particle vertex, and so forth.

For reasons too complex to try to explain I returned recently to an old fascination with $2 \to 3$ particle processes. I will describe here some of the problems we have tried to resolve in this domain at Argonne during the past half year or so.

2. EXCLUSIVE DIFFRACTIVE PROCESSES AND THE DECK MODEL

Many but not all of my remarks pertain to so-called diffractive processes, among which I may list

$$pp \to p(n\pi^+) \qquad 1(a)$$

$$np \to (p\pi^-)p \qquad 1(b)$$

$$pp \to p(\Delta^{++}\pi^-) \qquad 1(c)$$

$$\pi p \to (\pi\rho)p \qquad 1(d)$$

$$Kp \to (K^*\pi)p \ . \qquad 1(e)$$

For convenience of notation, and to call attention to the similarity of all of these, I write

$$ap \to (a^*\pi)p \ . \qquad 1(f)$$

Variables are defined in Fig. 1(a). Here a is an incident hadron from the set $K^\pm$, $\pi^\pm$, K^0, $\overline{K^0}$, p, $\bar{p}$, n and so forth. The related charge-exchange processes such as

$$K^-p \to (K^{*-}\pi^+)n \ . \qquad (2)$$

should be treated at the same time.

In reactions (1), the excited system is indicated in parentheses. The cross-section is concentrated at relatively small mass M of this system,

$M < 2$ GeV, although the excitation spectrum may well extend to very high values. Resonances may be present in the data as well as a broad continuum. In analyzing such reactions as effective quasi-two body processes, one usually defines a quasi-elastic differential cross-section in terms of the momentum transfer t to the isolated proton. The cross section is confined sharply to small t values.

The Deck model[3] has been used extensively to interpret the production and decay characteristics of non-resonant low-mass enhancements in the $(a^*\pi)$ system in reactions of type 1(f). In the model, exchange graphs of the type shown in Figs. 2(a) and 2(b) are used to describe the production amplitude at small values of the $(a^*\pi)$ mass. The use of exchanges in the "t-channel" and/or in the "u-channel" to describe scattering at low $(a^*\pi)$ subenergy deserves some justification, inasmuch as it is not an overwhelmingly successful methodology is $2 \to 2$ reactions. I doubt whether a good theoretical case can be made for or against. However, we can ask some pertinent questions of the data.

3. EXCHANGE MODEL DESCRIPTION AT LOW SUBENERGY

To what extent are we justified in using a model of t and/or u channel exchanges to describe the behavior of the amplitude when one of the subenergy variables is small? To narrow this question, it can partially recast as:

1. Are there features of data which give evidence of t and/or u channel exchange terms?
2. If so, can we learn about the quantum numbers of these exchanges by some simple tests?

I believe we have found positive answers to both of these questions. As a result, double-peripheral or double-Regge fits to data can be put on a more concrete foundation.

3.1. The S-Channel Azimuthal Angle

To answer the first question, we must find the "right" variable in which to display the data and thus bring out the desired information. Fortunately, the right variable is not a new complicated one, which no one will understand, and for which a long-series of uninspiring Monte Carlo simulations must be made. The "right" variable is an old and well-understood one. It is a helicity angle ϕ_s, defined with respect to an s-channel set of axes. Let us take as an illustration the reaction

$$ap \to a^*\pi N \ .$$

We want to investigate the behavior at small masses of the $(a^*\pi)$ system. We select as independent variables the natural set

$$s,\ s_{a^*\pi},\ t_{pN},\ \theta_s,\ \phi_s$$

where $(\theta_s,\ \phi_s)$ are decay angles of the $(a^*\pi)$ system, in its own rest frame. The direction of the final state N is the z axis. These variables are illustrated in Fig. 3.

Next, we must indulge in a small amount of kinematics. First, 2 to 3 particle phase-space when expressed in terms of the above set is

$$d\phi_3 = \prod_{i=1}^{3} \frac{d^3p_i}{(2p_{i0})}\,\delta(p_a + p_p - p_1 - p_2 - p_3)$$

$$= \frac{\pi}{16m_p|\vec{p}_a^{\,lab}|}\left(\frac{q}{\sqrt{s_2}}\right) dt_1 ds_2 d\cos\theta d\phi \ , \qquad (10)$$

where

$$2q\sqrt{s_2} = \{s_2 - (M_\pi + M_{a^*})^2\}^{\frac{1}{2}} \{s_2 - (M_\pi - M_{a^*})^2\}^{\frac{1}{2}} .$$

This equation tells us directly that in the absence of explicit dynamical dependence in the amplitude on this variable, the distribution $d\sigma/d\phi_s$ is flat over the fully allowed kinematic range: $0 \leq \phi_s \leq 2\pi$; or, when folded, $0 \leq \phi_s \leq \pi$. This is true regardless of cuts, biases, and/or dependence on the other four independent kinematic invariants in the set containing ϕ_s. Any structure in the plot $d\sigma/d\phi_s$, unless associated with ϕ_s biases, is therefore dynamical in origin, and teaches us about the production amplitude itself.

The second kinematic point also leads directly to conclusions of dynamical interest. Production amplitudes such as those shown in Fig. 2(a) and (b) tend to depend on Lorentz-invariant kinematic subenergy and momentum transfer quantities and not on θ_s and ϕ_s directly. These subenergy and momentum transfer variables (not included in our basic set above) can be expressed as

$$s_{\pi N} = A_1 + B_1 \cos\theta_s \tag{11}$$

$$s_{a^*N} = A_2 - B_1 \cos\theta_s \tag{12}$$

$$t_{aa^*} = a_1 + b_1 \cos\theta_s + c_1 \sin\theta_s \cos\phi_s \tag{13}$$

$$u = t_{a\pi} = a_2 - b_1 \cos\theta_s - c_1 \sin\theta_s \cos\phi_s . \tag{14}$$

The functions A_1, A_2, B_1, a_1, a_2, b_1 and c_1 depend on s, $s_{\pi a^*}$, and t_{pN}, only. Explicit expressions for them are given in Ref. 3. Here we need to notice only some simple facts:

(i) the subenergy variables do not depend on ϕ_s;

(ii) the momentum transfer variables t_{aa^*} and $t_{a\pi}$ depend linearly on $\cos\phi_s$. Given the choice of axes I made in

Fig. 3, $(-t_{aa^*})$ has its minimum value when $\phi_s \to 0$, $\cos\phi_s \to +1$, and $(-t_{a\pi})$ has its minimum when $\phi_s \to \pi$, $\cos\phi_s \to -1$.

Therefore, as we vary ϕ_s from $\phi_s = 0$ to $\phi_s = \pi$, the dynamics changes from one in which small t_{aa^*} is important to one in which small $t_{a\pi}$ is the controlling influence. This is exactly the type of variable we need. The graph (a) in Fig. 2 is one whose amplitude is large when t_{aa^*} is small. The amplitude decreases in magnitude as $|t_{aa^*}|$ increases. On the otherhand, the amplitude for graph (b) is largest when $(-t_{a\pi})$ is its smallest. For the process $ap \to a^*\pi N$, therefore, the dynamics are controlled by t channel exchange near $\cos\phi_s = +1$ and by u channel exchange near $\cos\phi_s = -1$. We may expect to see peaks near $\cos\phi_s = \pm 1$ in the plot $d\sigma/d\phi_s$ corresponding to these two different exchange graphs. As an illustration of expected effects, one may examine the Fig. 4. In this figure I present simulated data obtained from a Monte Carlo calculation of the pion-exchange Deck graph.[3] It is clear that in both the diffractive and charge exchange cases, the pion exchange term populates the region $\phi_s < \pi/2$ very strongly. Details of the calculation may be found in Ref. 3.

Note, in passing, that the peak in $d\sigma/d\phi_s$ near $\phi_s = 0$ is the π exchange peak. The pion-pole is not cancelled in this variable, as it is in other plots, by the dependence of the inelastic amplitude on other variables. This should put an end to the loose talk in some recent literature regarding cancellation of pion singularity.

At small $M_{a^*\pi}$, there is considerable overlap in phase space of the small t_{aa^*} and small $t_{a\pi}$ regions. There is also overlap in the ϕ_s plot. We certainly cannot propose a neat cut at, say, $\phi_s = \pi/2$, to separate the two contributions. The overall appearance of the plot $d\sigma/d\phi_s$ will

reflect the relative cross-section associated with the t- and u-channel graphs. If the t-channel (u-channel) graph is overwhelming, there will appear to be only a general peaking of $d\sigma/d\phi_s$ near $\phi_s = 0(\pi)$. If the u-channel and t-channel graphs are comparable in size, the plot $d\sigma/d\phi_s$ could be relatively flat. The safest general statement is that the selection $\cos\phi_s > 0$ enhances the t-channel contribution whereas the selection $\cos\phi_s < 0$ enhances the u-channel exchange contribution.

3.2. Experimental Results

With the assistance of experimenters at CERN, I have been looking at some distributions of $d\sigma/d\phi_s$ for various reactions. For the charge exchange reaction

$$K^- p \to K^{*-} \pi^+ n ,$$

only a t-channel pion exchange type graph is expected. No u-channel graph exists since the u-channel has exotic quantum numbers. In the data at 4.2 GeV/c, only a peak near $\phi_s = 0$ is observed, as expected.[4] This result gives important qualitative support to the use of an exchange model description at very low subenergy ($M_{K^*\pi} < 1.3$ GeV). For $K^\pm p \to K^{*0} \pi^\pm p$, both t channel, pion exchange type graphs, and u-channel K^* exchange type graphs are possible.

A preliminary view of data in the Q region from $K^\pm p \to K^* \pi^\pm p$ at 8 GeV/c[5] and for $K^- p \to \overline{K^*} \pi^- p$ at 16 GeV/c[6] show rather flat $d\sigma/d\phi_s$ distributions. This result supports the conclusion that, in these reactions, the π and K^* exchange graphs are of roughly equal importance. This is the first direct evidence that the pion exchange Deck graph alone is incapable of reproducing the data in the Q region. Within the context of an exchange model interpretation of the Q enhancement, both "t-channel" (i.e., π) and "u-channel" (i.e., K^*) exchange graphs are required in roughly equal

proportion. In studies of $pn \to p(p\pi^-)$ at 19 and 28 GeV/c, the Brookhaven-Vanderbilt collaboration[7] finds a ϕ_s distribution in the low-mass $(p\pi^-)$ system which shows roughly a 2 to 1 ratio of events favoring π over baryon exchange.

More investigations of this type of the $d\sigma/d\phi_s$ plot would be of great assistance in establishing the qualitative exchange features of data at low subenergies in many other reactions, not confined to the diffraction dissociation class. Furthermore, selections on ϕ_s yield data samples in which the properties of one exchange channel (t or u) can be investigated with relatively reduced contamination from the other channel. An example of such use is described in the next section.

4. CROSS-OVERS

It is observed experimentally that the logarithmic slope b_- of $d\sigma/dt$ for π^-p elastic scattering is larger than b_+ for π^+p elastic scattering. At high energy the value of the π^-p differential cross-section at $t = 0$ is larger than that of π^+p, and its value at $|t| \gtrsim 0.4$ $(GeV/c)^2$ is smaller.[8] The cross-over occurs near $t \approx -0.2$ $(GeV/c)^2$. These cross-over properties of πN elastic scattering should be reflected in inelastic processes if the pion exchange Deck model is relevant.

The π exchange Deck graphs relevant for $\pi^\pm p \to (3\pi)^\pm p$ and $K^\pm p \to (K\pi\pi)^\pm p$ are sketched in Fig. 5. It will be noted that $d\sigma/dt'$ for the $\pi^\pm$ (and $K^\pm$) induced inelastic processes is controlled by $\pi^\pm$ elastic scattering. Thus, we easily predict $b_{K^-} > b_{K^+}$ and $b_{\pi^-} > b_{\pi^+}$ for the above inelastic reactions, in fine accord with data.[9,10]

The analogous expectation for neutral Q production does not agree with experiment.[11] As sketched in Fig. 6, the process $K^0p \to Q^0p$ is a reflection of π^-p elastic scattering, whereas $\bar{K}^0p \to \bar{Q}^0p$ reflects π^+p.

Thus, $b_{K^0} > b_{\bar{K}^0}$ is the π-exchange Deck model expectation. Data from a SLAC experiment show the opposite.[11] The SLAC $K^0p \to Q^0p$ results agree with the general systematics abstracted from elastic processes, which is that anti-particle induced reactions have larger values of $d\sigma/dt$ at $t = 0$ and larger slopes than their particle induced counterparts.[8]

What are the implications of the disagreement with the SLAC data? One interesting conclusion within the Deck model context is that a K^* exchange graph must be involved. The K^*p (off-shell) elastic scattering presumably obeys canonical systematics, with $b_{\bar{K}^*} > b_{K^*}$. As a reflection, in the inelastic process $K^0p \to Q^0p$, we expect $b_{\bar{K}^0} > b_{K^0}$. Inspection of the ϕ_s plot, discussed above shows that the π and K^* exchange graphs <u>both</u> contribute to $K^+p \to Q^+p$. For $K^-p \to Q^-p$, the π and K^* exchange graphs give the same prediction $b_{K^-} > b_{K^+}$, in agreement with data. However, for $K^0p \to Q^0p$, the two graphs give opposite results. The K^* exchange graph dominates the cross-over for $Kp \to Qp$, presumably because the cross-over effect is more pronounced in Kp elastic scattering than in πp elastic.

The reaction $K^0p \to Q^0p$ is not the only reaction for which the π exchange Deck graph and the "other" exchange graph would predict opposite signs for cross-overs in $d\sigma/dt'$. In Table 1 of Ref. 12 I itemize a set of reactions and list the cross-over systematics expected. The overall cross-over in the data, if any, is determined by the relative weights of the two contributing exchange amplitudes.

<u>Selections</u> on ϕ_s should be especially useful.[12] If events are chosen with $\cos\phi_s > 0$, the contribution from the π exchange Deck graph is enhanced. Correspondingly, $\cos\phi_s < 0$ selects the K^* exchange graph.

Returning to the cross-over situation in $K^0p \to Q^0p$, I predict that events in the $\cos\phi_s > 0$ segment should have the non-canonical cross-over

behavior $b_{K^0} > b_{\bar{K}^0}$, controlled by the π exchange graph, whereas events with $\cos\phi_s < 0$ should follow the K^* exchange systematics, $b_{\bar{K}^0} > b_{K^0}$. If this prediction fails, the Deck model is in serious difficulty.

A second reaction for which there are data is $\pi^\pm p \to \pi^\pm(\pi^-\Delta^{++})$ at 16 GeV/c.[9] No cross-over is observed in the total sample. Here ϕ_s is the helicity angle of the Δ^{++} in the $(\pi^-\Delta^{++})$ rest frame. Events with $\cos\phi_s > 0$ should have a cross-over determined by $(\pi^\pm\pi^-)$ elastic scattering, namely $b_{\pi^+} > b_{\pi^-}$. If $\cos\phi_s < 0$, the Deck graph incorporates $(\pi^\pm\Delta^{++})$ elastic scattering, for which $b_{\pi^-} > b_{\pi^+}$ is expected. The overall absence of a cross-over suggests equal compensating contributions from the π and Δ exchange graphs. These predictions[12] were checked in the data by making the ϕ_s selections and examining the cross-over properties of the t-distributions in the two segments. The predictions are confirmed.[13] The same predictions apply to $K^\pm p \to K^\pm(\pi^-\Delta^{++})$, for which data exist at 8 GeV/c.[5]

The success of the cross-over predictions for $\pi^\pm p \to \pi^\pm(\pi^-\Delta^{++})$ confirms the utility of the $\cos\phi_s$ selection procedure. It also helps to establish that the $\cos\phi_s > 0$ region shows quantum number characteristics (symmetry properties) of π exchange, whereas the $\cos\phi_s < 0$ region has baryon exchange properties. Thus, the validity of using exchanges of specific type to describe the low mass $(\pi^-\Delta^{++})$ enhancement is supported. Note, in passing, that the data show also that production and decay of $(\pi^-\Delta^{++})$ do not factorize, in that different portions of the decay angular distribution have different production characteristics.

5. A DIFFERENT RESOLUTION OF THE Q CROSS-OVER PROBLEM

Cohen-Tannoudji and collaborators[14] at Saclay have found a different theoretical way to explain the cross-over problem[11] for $K^0p \to Q^0p$ and

$K^o p \to \bar{Q}^o p$. They do not invoke K^* exchange. Rather, they add the graph drawn in Fig. 7, to the usual π exchange Deck amplitude. Their extra term involves B and ω exchange. At $t = 0$, it adds constructively to $K^o p \to \bar{Q}^o p$, but destructively to $K^o p \to Q^o p$. The cross-over arises because the $B\omega$ term and the πf piece of Fig. 6 cancel each other at the cross-over point. I find this explanation difficult to accept, because I do not expect the $B\omega$ amplitude to be large enough to do the job and because it requires too delicate a balance of phases. In any case, the $\cos\phi_s$ selection procedure I described above allows us to test the scheme.

According to the Cohen-Tannoudji ansatz[14], the cross-over should be the same over the whole $\cos\phi_s$ region, even in the region $\cos\phi_s > 0$ where π exchange is enhanced. According to my K^* exchange solution described above, the cross-over in the region $\phi_s < \pi/4$ where π exchange dominates, should obey $d\sigma/dt\ (K^o) > d\sigma/dt\ (\bar{K}^o)$, at $t = 0$, and slope K^o greater than slope $\bar{K}^o$, contrary to the full data sample. The decision is up to the experimenters at SLAC who have the tapes.

6. RESONANCE-DECK INTERFERENCE

The Deck amplitude provides a low mass enhancement whose partial wave content covers a series of spin-parity states. In Nature, there may also be, in addition, resonances in some or all of these waves, whose production is coherent with that of the non-resonant (Deck) background. For instance, in $\pi p \to (3\pi)p$, there is the $J^P = 2^+$ A_2 resonance (d wave $\rho\pi$), which may interfere with the Deck 2^+ wave.

It is interesting to inquire about possible resonances in the s wave (πa^*) system, which would interfere with the dominant s wave produced in the Deck model. Cross-section estimates for the production of such resonances

run in the 10 to 20 μb range[15], whereas the Deck background is of order 100 μb. Thus, the resonances would not stand out clearly in standard plots of invariant mass. Moreover, existing three particle phase shift analysis programs may find it particularly hard to disentangle such a weak resonance signal from the Deck background.

The resonances might well show up more transparently if the mass distribution $d\sigma/dM_{\pi a^*}$ were plotted for events from a partial segment of the decay angle phase space. Specifically, one might consider displaying events in the two dimensional decay space defined by $(\cos\theta_t, \phi_t)$ [or by $(\cos\theta_s, \phi_s)$]. Here $[\cos\theta_t, \phi_t]$ are t channel decay angles, with the quantization axis along the direction of incident particle a. The events could be divided into four (eight) samples and plots of $d\sigma/dM_{\pi a^*}$ made for each:

$$\begin{aligned} &\text{I.} && -1 \leq \cos\theta \leq 0 && \pi \geq \phi \geq \pi/2 \\ &\text{II.} && -1 \leq \cos\theta \leq 0 && \pi/2 > \phi \geq 0 \\ &\text{III.} && 0 < \cos\theta \leq 1 && \pi \geq \phi \geq \pi/2 \\ &\text{IV.} && 0 < \cos\theta \leq 1 && \pi/2 > \phi \geq 0 \end{aligned} \qquad (15)$$

A single resonance would populate all four (eight) segments equally, whereas the π exchange and a^* exchange Deck graphs concentrate events towards specific corners, as shown in Fig. 8. The character of the resonance-Deck interference should be sufficiently different in the four sectors. If events taken, for example, from the two non-Deck corners of the $(\cos\theta, \phi)$ plot were to show statistically significant, relatively narrow structure, the case for resonance interpretation would be correspondingly strengthened. Background graphs do not create narrow peaks. Selection procedures similar to these seem to have been useful in analyses of ISR and FNAL diffraction dissociation data.[16,17]

In searching for resonance effects in the $Q(K\pi\pi)$ region, careful comparisons of K^+p and K^-p data may be particularly illuminating. Because the K^+p channel is exotic whereas K^-p is not, the relative phase of resonance and Deck background should be different in the two cases. This phase difference might explain the different mass structure observed for the Q^+ and Q^-.

7. EFFECTS OF ABSORPTION IN INELASTIC REACTIONS

Notable contrasts are apparent when the (quasi-elastic) t dependence of $d\sigma/dt\,dM$ for reactions 1(a) and 1(b) is compared with that of $d\sigma/dt$ for elastic scattering. In elastic scattering at ISR energies[18], $d\sigma/dt$ falls in featureless, roughly exponential fashion by over 6 orders of magnitude from its maximum at $t = 0$, before encountering a sharp minimum at $|t| \approx 1.4$ $(GeV/c)^2$. When recast in impact parameter language, these data imply that diffractive elastic scattering is a central process[18], concentrated about zero impact parameter. In contrast, in inelastic diffraction at small values of excitation mass, M, Fermilab data[17] on reaction 1(b) and ISR data[16] on reaction 1(a) show a dip or at least a break in $d\sigma/dt\,dM$ at $|t| \approx 0.2$ $(GeV/c)^2$, (after a precipitous fall from the maximum at $t = 0$). A dip at such small $|t|$ implies peripheral structure in impact parameter[19], with the cross-section peaking at about 1 fermi. Although a break near $|t| \approx 0.2$ $(GeV/c)^2$ had been observed in some lower energy data[20], below 30 GeV/c, the possibility existed that the effect was a non-asymptotic, non-diffractive phenomenon. The ISR and Fermilab results demonstrate the diffractive nature of the inelastic structure. They compel the conclusion that quasi-elastic scattering is peripheral in impact parameter, whereas elastic scattering is central.

These new results are not reproduced by the unabsorbed pion-exchange Deck model which had provided a successful picture of many features of earlier data. In particular, according to the model,[3] the distribution in momentum transfer to the diffractively scattered proton should resemble that for elastic scattering, thus showing no structure at $|t| \simeq 0.2$ (GeV/c)^2 in reactions 1(a) and 1(b). A related problem concerns the variation with mass M of the small t slope of $d\sigma/dt\,dM$. A marked decrease of slope is observed in the data as mass M is increased above the threshold value $(m_\pi + m_n)$. While explained qualitatively by the model, this "mass-slope" correlation has not always been satisfactorily reproduced quantitatively in calculations to date.[21]

In addition to these difficulties in practice, there are questions of principle which lead one to reexamine the model. In inelastic two-body and quasi-two body reactions, absorptive corrections[22] are found to be often important. Such effects should a priori be included also in a proper calculation of two to three body reactions of the type (1). The role, indeed, necessity of such absorption terms is further apparent when one adopts the optical interpretation of diffraction dissociation.[23] Since absorptive effects in 2 body reactions often lead to structure near $|t| \simeq 0.2$ (GeV/c)^2 in s-channel non-spin flip amplitudes[22], the motivation for seeking an absorptive explanation of the structure in inelastic diffraction dissociation is increased.

7.1 An Explicit Model

In a recent paper,[24] P. Pirila and I construct an explicit absorbed pion exchange Deck model for reactions 1(a) and 1(b). We achieve good agreement with the recent FNAL and ISR data.[16,17] Our results support

the Deck interpretation of diffractive threshold enhancements, as well as the necessity for absorptive corrections to the model.

The unabsorbed pion-exchange Deck amplitude which we employ in our calculations is the stripped-down expression

$$A_0(s_1,t_2,t_1) = i\, g_\pi\ (t_2)\ \sigma^{\pi p} s_1\ \exp(B_1 t_1)\ . \tag{16}$$

The factor $i\, s_1\, \sigma^{\pi p} \exp(B_1 t_1)$ represents the essential subenergy and exponential momentum transfer dependence of the (off-shell) πp diffractive elastic scattering amplitude imbedded in the unabsorbed amplitude, Fig. 2(a); $\sigma^{\pi p}$ is the total πp cross-section. The function $g_\pi(t_2)$ is the pion propagator and coupling function. Explicitly,

$$g_\pi(t_2) = \sqrt{2}\ g\ \sqrt{-t_2}\ \exp(t_2 - M_\pi^2)/(M_\pi^2 - t_2)\ . \tag{17}$$

We ignore Reggeization of the pion, which would introduce dependence on s_2 into Eq. (16), as well as a t_2 dependent phase variation. These omissions are in essential to the major conclusions of our investigation.[24]

Arguments based on both the optical approach to diffraction dissociation and the double-peripheral model lead to the conclusion that the important absorptive amplitude A_{abs} is the "final state" rescattering term, represented in Fig. 9. This is correct to the extent that the ratio $(M_{a^*\pi}/\sqrt{s})$ is a small parameter, which is true for low mass diffractive excitation. We use on-shell propagators for the intermediate state particles a^* and p. Detailed arguments are presented in Ref. 24. We adopt a conventional asymptotic exponential parametrization of the elastic final state rescattering

$$A_{el}^{a^*p}(s_{12},t_3) = i\, s_{12}\, \sigma^{a^*p} \exp(B_3 t_3)\ . \tag{18}$$

$$s_{12} = (p_1 + p_2)^2\ . \tag{19}$$

A loop integral must be done to evaluate A_{abs}. After some uninspiring algebra and integrating to remove two mass-shell delta functions, consistently dropping correction terms of order $(M_{a^*\pi}/\sqrt{s})$, we obtain

$$A_{abs} = \frac{i}{8\pi^2 s_{12}} \int d^2\vec{q}_{3T} A_{el}^{a^*p}(s_{12},t_3)\, A_0(s,t_1',t_2',s_1',s_2') \quad . \tag{20}$$

with

$$t_3 = -\vec{q}_{3T}^{\,2} \tag{21}$$

$$t_1' = t_1 - (\vec{q}_{3T}^{\,2} + 2\vec{q}_{3T} \cdot \vec{p}_{1T}) \tag{22}$$

$$t_2' = t_2 - \frac{1}{x_2}(\vec{q}_{3T}^{\,2} - 2\vec{q}_{3T} \cdot \vec{p}_{2T}) \tag{23}$$

$$x_2 = p_{2L}/p_{cm} = 2p_{2L}/\sqrt{s} \tag{24}$$

$$s_1' = s_1 + \vec{q}_{3T}^{\,2}\,(1 - \frac{1}{x_2}) + 2\vec{q}_{3T} \cdot (\vec{p}_{1T} + \frac{1}{x_2}\vec{p}_{2T}) \quad . \tag{25}$$

The two-dimensional transverse vectors $\vec{p}_{1T}$ and $\vec{p}_{2T}$ are the transverse components of the momenta of final state particles p and a^*, respectively; p_{2L} is the center of mass longitudinal component of a^*. The Eq. (20) rather general, independent of the specific choices for A_0 and A_{el} made above.

We substitute Eqs. (16) and (18) into Eq. (20), and we define a new variable for convenience:

$$\vec{v} = \vec{p}_{2T} + \frac{B_1}{(B_1 + B_3)}\vec{p}_{1T} \tag{26}$$

After minor algebraic manipulations and a change of integration variables, we perform an angular integration analytically. The result is a one dimensional integral expression for A_{abs}.

$$A_{abs}(s_1,t_2,t_1) = \frac{-\sigma a^* p}{8\pi} \frac{A_0(s_1,t_2,t_1)}{g(t_2)} \exp\left[\frac{-B_1^2 t_1}{B_1+B_3} - (B_1+B_3)\vec{V}^2\right]$$

$$\times \int dU^2 \, I_0\left[2(B_1+B_3)U|\vec{V}|\right] g(t_2') \exp(-(B_1+B_3)U^2) \qquad (27)$$

$$t_2' = t_2 + \frac{1}{|x_2|}(\vec{p}_{2T}^2 - U^2)$$

$$= -\frac{1}{|x_2|} U^2 + m_a^2(1-|x_2|) + m_{a^*}^2(1-1/|x_2|) \; . \qquad (28)$$

In Eq. (27), the function I_0 is a modified Bessel function. It enjoys the properties

$$I_0(\chi) \to 1 \quad \text{as} \quad \chi \to 0$$

and

$$I_0(\chi) \to \exp(\chi)/\sqrt{2\pi\chi} \quad \text{as} \quad \chi \to \infty \; .$$

The expression (27) for A_{abs} contains a one dimensional integral which must be evaluated numerically.

In interpreting Eq. (27), it is useful to notice that to leading order in s, the momentum transfers t_1 and t_2 are given by ($|x_1| = 1$)

$$t_1 = -\vec{p}_{1T}^2 \; . \qquad (29)$$

$$t_2 = -\frac{1}{|x_2|}\vec{p}_{2T}^2 + m_a^2(1-|x_2|) + m_{a^*}^2(1-1/|x_2|) \; . \qquad (30)$$

Therefore, the exponential factor in Eq. (27) is an increasing function of $(-t_1)$ and $(-t_2)$. We observe directly the expected result that the double scattering or absorption amplitude has a weaker dependence on t_1 and t_2 than the unabsorbed amplitude. Since the two amplitudes differ in sign, cancellation occurs in the full amplitude

$$A = A_0 + A_{abs} \; . \qquad (31)$$

A zero of A is generated at well defined values of t_1 and t_2.

We now select the specific dissociation process $pp \to p(n\pi^+)$ at 100 GeV/c in order to specify parameters. For small values of $M_{n\pi^+}$, the typical value of $\sqrt{s_1}$ is $\sqrt{s/2}$ and $s_{12} \approx s$. Thus, the elastic scattering parameters $B_1 = 4.5$ (GeV/c)$^{-2}$ and $B_3 = 5.5$ (GeV/c)$^{-2}$ are reasonable, with $\sigma^{np} \approx 38$ mb = 98 GeV^{-2}. Because these parameters are taken directly from measured elastic and total cross-section data, the dip positions we calculate for $d\sigma/dt\, dM$, and the slopes are absolute predictions. In Figs. 10 and 11, and Table I, I compare results obtained from our unabsorbed and absorbed models for $pp \to p(n\pi^+)$ at 100 GeV/c. The same apply to $np \to (p\pi^-)p$.

7.2. The Momentum Transfer Distribution

The most dramatic effect of absorption is observed in the momentum transfer distribution $d\sigma/dM\, dt$ for production of the low-mass diffractive enhancement. I select the mass value $M_{n\pi^+} = 1.3$ GeV because this corresponds roughly to the center of the peak in mass generated by the model. In the unabsorbed model, Fig. 10(a), $d\sigma/dt_1$ falls roughly exponentially, whereas in the absorbed model, Fig. 10(b), a pronounced break structure is observed near $|t| \approx 0.4$ (GeV/c)^2. This structure is caused by the cancellation between A_0 and A_{abs} in Eq. (31).

Near the threshold value $M = (m_N + m_\pi)$, $d\sigma/dt\, dM$ shows a pronounced dip near $|t| = 0.3$ (GeV/c)^2 in the model. This dip gradually transforms into the break structure seen in Fig. 10(b). Perceptible structure disappears altogether at higher M. These results agree at least qualitatively with experiment.[16,17]

We decomposed our full amplitude for the process $pp \to Mp$ into partial amplitudes for each of the angular momentum and helicity states which con-

tribute to the system M. We investigated how absorption affects each of these partial amplitudes individually. In Fig. 10, for both the absorbed and unabsorbed differential cross-section, we show the total $d\sigma/dt\,dM$, as well as a decomposition of this quantity, into the portions for each of the spin and helicity states which contribute to the system of mass M. Indeed, the recoil system M in $pp \to pM$ is not in a state of unique spin, although the s-wave component is certainly dominant. Our Deck amplitudes specify the relative strengths of the different spin states. In Fig. 10, the partial wave decomposition is presented in terms of s-channel helicities of system M (the quantization z axis is the direction of the final proton). We have ignored intrinsic spins of particles. Therefore the spin, helicity labels refer to orbital angular momentum only in the rest system of M. The quantity labeled σ^{11} is the sum of σ^{11} and $\sigma^{1,-1}$.

A comparison of Figs. 10(a) and 10(b) shows that the amplitudes with s-channel helicity $|\lambda_s| \geq 1$ are not much absorbed. The states with $\lambda_s = 0$ suffer the greatest absorption. At $M_{\pi^+n} = 1.3$ GeV, in the state $[L = 0, \lambda_s = 0]$, a zero of the full amplitude is generated at $|t| = 0.37\ (\mathrm{GeV/c})^2$. The zero locations of some other amplitudes are listed in Table I, for three values of mass. These explicit zero locations correspond crudely but not exactly to positions conjectured in ad-hoc geometric models.[19,25] Most notable is the fact that all zero locations move to larger $|t|$ as M increases. In impact parameter language, this means that for fixed (L,λ) states of higher mass are produced less peripherally in our model. As a result of this motion of the zero location with M, structure in $d\sigma/dt\,dM$ is washed out if a relatively large interval (e.g. $\Delta M \gtrsim 0.5$ GeV) in M is averaged or integrated over. Thus, even $d\sigma^{L,\lambda_s}/dt\,dM$ for a specific $[L,\lambda_s]$ state may show little or no structure in t if too large an interval in M

is selected in the data. High statistics data with good mass resolution are crucial.

In Fig. 10(b) we note that the $[L = 1, \lambda_s = 1]$ amplitude fills in the pronounced dip in $d\sigma/dt$ near $t = 0.4$ $(GeV/c)^2$ which would occur if only the $[L = 0]$ state were present. The dip is partially removed by a state of different s-channel helicity. In the unabsorbed results, Fig. 10(a), the ratio σ^{00}/σ^{11} is roughly 6 at $|t| = 0.4$ $(GeV/c)^2$. However, roles are entirely reversed in the absorbed model, with the $[L = 1, \lambda_s = 1]$ state being overwhelming near this value of $|t|$.

It is useful to recast the results of the above paragraphs in impact parameter language. The elastic scattering amplitude and the unabsorbed π exchange Deck amplitude have roughly exponential dependence on momentum transfers t_3 and t_1', respectively. (c.f. Eqs. (16) and (18). Therefore, both are approximately Gaussian functions of impact parameter, and represent "central" collisions. Absorption generates a zero at $t_1 \simeq -0.3$ $(GeV/c)^2$, as discussed. When translated to impact space, this means that the central partial waves are depleted. At small values of the mass of the excited system, the resulting diffractive inelastic absorbed Deck amplitude has a peripheral impact parameter structure.

7.3. Mass-Slope Correlation

In Fig. 11 we present the variation with $M_{n\pi^+}$ of the small t slopes of $d\sigma/dt\, dM_{n\pi^+}$. The slope b is defined through the parametrization

$$\frac{d\sigma}{dt\, dM} \propto \exp(bt) \ .$$

Fits were made over the range $0.05 \leq |t| \leq 0.2$ $(GeV/c)^2$. The comparison of absorbed and unabsorbed results in Fig. 11(a) indicates that absorption increases the threshold value of the slope by roughly 9 units, but causes

only a modest increase at $M_{n\pi^+} \simeq 2$ GeV. Absorption accentuates the pronounced mass-slope correlation already present in the unabsorbed model. On Fig. 11(a) we have placed slope values obtained in a recent Fermilab experiment[17] on $np \to (p\pi^-)p$. The excellent agreement with our absolute predictions in the mass range up to 1.4 GeV seems to support strongly the Deck interpretation of kinematic nature of low-mass threshold enhancement, as well as the need for absorptive corrections in the model. At larger $M_{p\pi^-}$, from 1.5 to 2.0 GeV, the model disagrees with data.[17] However, we call attention to the fact that in this region, obvious resonance effects are observed in the data. They are not included in the model. The resonances appear to be produced with a t slope which is substantially smaller than that of the diffractive Deck background.

In Fig. 11(b), we present the slope of $d\sigma^{00}/dt\, dM$. This is the differential cross-section for producing the s-wave part only of the Deck enhancement. We observe that there is a pronounced mass-slope correlation in both the unabsorbed and absorbed results. Although perhaps of somewhat esoteric interest now, we include these results in the expectation that data will soon be available. The results of Fig. 11(b) demonstrate that in our model the mass-slope correlation is present already in the dominant $L = 0$ partial wave, all by itself.

An alternative interpretation[19,25] of the mass-slope correlation has been suggested repeatedly. In these approaches, the mass-slope correlation owes its existence to the presumed growth with M of higher L and λ_s states, produced with systematically smaller slopes b. For a given (L,λ_s), the slope b is assumed not to vary with M. While perhaps intuitively appealing, the approach suffers from a surplus of undetermined parameters and has not been tested quantitatively. It seems to us unlikely that the

data (particularly the distribution in ϕ_s) would tolerate an increase of λ_s with M sufficiently rapid to achieve the result desired. In any case, the issue can be resolved experimentally. Some data on the mass-slope correlation in the L = 0 partial wave in $\pi p \to (\rho\pi)p$ at 40 GeV/c have been published.[26] A decrease of slope from 12 ± 1 to 7 ± 1 $(GeV/c)^{-2}$ is observed [c.f. Table 1, p. 157 of Ref. 26] from $M_{\rho\pi} = 1.1$ to 1.3 GeV. Therefore, available results, while sketchy, surely are consistent with our viewpoint that the mass-slope correlation is an intrinsic property of each partial wave.

The mass-slope correlation arises in the pion exchange Deck model from a convolution of momentum transfer dependences. This is true also of the absorbed model. The mechanism can be tested by analyzing the data in the full four-dimensional space.[21] In the model, this effectively removes the convolution effect.

It has been found that the variation of slope with mass in the data is essentially the same for the two methods. Thus, the model explanation is at best incomplete. It works for $d\sigma/dt_1 dM$, but it fails in the four dimensional analysis. Absorption does not remedy the problem. As far as we can determine, no model in the literature has been shown to survive the four-dimensional test. We believe that the mass-slope correlation effect in the full four dimensional space can be obtained properly only after both the u-channel and t-channel graphs Fig. 2(a and b) are included in the calculation. Preliminary analyses verify this conjecture. We expect to report the results elsewhere.

7.4. Other Effects of Absorption

As just summarized, the most dramatic effects of absorption are seen in the production t distribution $d\sigma/dM\,dt$. The integrated mass distribution

$d\sigma/dM$ shows little modification in shape in the small M region of interest here. Absorption does not yield the sharpening effect which might be desirable in improving fits to data on $d\sigma/dM$. The overall integrated cross-section is reduced to roughly one-half its unabsorbed value. At small t, the decay angular distributions in the rest frame of M are essentially unchanged by absorption. At larger $|t|$, [$\gtrsim 0.3$ $(GeV/c)^2$], where the absorption term and the unabsorbed amplitude are of comparable magnitude, the predicted partial wave structure is modified appreciably. The Fig. 10 may be consulted for numerical estimates. Insofar as statistics allow, it is advisable to perform experimental partial wave analyses of the system M in several different regions of $|t|$. If all t values are included, little difference is seen between the absorbed and unabsorbed models.

Because meson-nucleon total cross-sections are smaller than σ^{np}, we expect absorptive effects to be less important in diffractive reactions induced by a meson beam, e.g. $\pi p \to A_1 p \to (\rho\pi)p$; $Kp \to Qp \to (K^*\pi)p$; and $\pi p \to \pi(N\pi)$. The position of the dip or break in $d\sigma/dt_1$ moves out to larger $|t_1|$, as shown explicitly in Ref. 24.

Certain predictions based on the unabsorbed Deck model must be reevaluated in the light of our present conclusion that absorptive corrections are necessary. Several of these issues have already been treated above. We include brief remarks here on two other questions. Nucleon polarization effects were discussed by Berger and Fox.[27] As a result of absorption, the effective Pomeron in inelastic diffraction has structure in t which is considerably different from that in elastic scattering. The inelastic Pomeron amplitude passes through zero near $|t| = 0.3$ $(GeV/c)^2$, whereas the elastic Pomeron amplitude is apparently featureless out to $|t| \approx 1$ $(Gev/c)^2$. This structure is reflected in the t dependence of the inelastic polarization.

Thus, rather than the positive polarization, with a double-zero near $|t| \simeq 0.6$ (GeV/c)^2, expected previously[27] for $pp \to p(n\pi^+)$, we now expect a change of sign of polarization from positive to negative near $|t| = 0.3$ (GeV/c)^2. These modifications are sketched in Fig. 12. The location of this zero moves to larger $|t|$ as $M_{n\pi^+}$ is increased. When integrated over $|t|$, the polarization as a function of $M_{n\pi^+}$ will also be smaller, owing to this sign change. This may explain the small polarization observed in inclusive reactions $pp \to px$ at small M_x. We can only urge again that detailed polarization data as a function of t and M in selected exclusive inelastic diffraction dissociation processes should be of great assistance in further defining the dynamics of quasi-elastic reactions. Experiments with the Argonne polarized proton beam are of obvious interest.

The second remark pertains to cross-overs in t of the differential cross-sections observed when data are compared for pairs of reactions related by charge-conjugation in the t-channel. This subject was discussed above in Section 4 in the context of the unabsorbed Deck model. An interesting example is the pair $K^o p \to Q^o p$ and $\overline{K^o} p \to \overline{Q^o} p$, for which the unabsorbed pion exchange Deck graphs are given in Fig. 6. These pion-exchange Deck graphs predict that at $t = 0$, $d\sigma/dt\ (K^o) > d\sigma/dt\ (\overline{K^o})$, because $\sigma(\pi^- p) > \sigma(\pi^+ p)$. They also predict that the slope of $d\sigma/dt\ (K^o)$ > slope of $d\sigma/dt\ (\overline{K^o})$, because this is true of the slopes of the $\pi^{\pm} p$ elastic scattering amplitudes which are imbedded in the Deck graphs. These two expectations disagree with data[11], for which just the opposite results are true.

Absorption involves rescattering of the final $K^* p$ and $\overline{K^*} p$ systems. Because the non-exotic $K^{*-} p$ total cross-section is presumably greater than the exotic $K^{*+} p$ total cross-section, just as $\sigma^{K^- p} > \sigma^{K^+ p}$, we expect the absorptive effects to be stronger in the $\overline{K^o} p$ reaction than in $K^o p$.

These reduce the $t = 0$ value of the $\overline{K^0}p$ cross-section relative to that for K^0p. Unfortunately, this goes in just the wrong direction to remedy one of the discrepancies with the data. Absorption increases the slope of $d\sigma/dt$ $(\overline{K^0})$ relative to that of $d\sigma/dt$ (K^0), counteracting the tendency of the unabsorbed amplitude, but its effect on the magnitude of the cross-section destroys the cross-over. In our view[12], a proper description of the cross-over requires including both the K^* and π exchange Deck amplitudes. This conclusion is, if anything, strengthened by our present demonstration that absorption alone is not the answer to the cross-over problem.

8. CONCLUSIONS

Selections on the s-channel azimuthal angle of a^* [in the $(a^*\pi)$ rest frame] were proposed to separate the regions of phase space in which the t-channel pion exchange and u-channel a^* exchange Deck graphs dominate the amplitude for $ap \to (a^*\pi)p$, at small values of the $(a^*\pi)$ invariant mass. The pion exchange Deck amplitude produces a distribution $d\sigma/d\phi_s$ which peaks sharply towards $\phi_s = 0$. This property is intimately associated with the t-channel exchange property of Deck graphs. A u-channel graph, having a ρ or K^* exchange, provides a peak towards $\phi_s = \pi$. The quantum number characteristics of π exchange (a^* exchange) should prevail only in the region $\cos\phi_s > 0$ ($\cos\phi_s < 0$).

Data on several reactions show that although $d\sigma/d\phi_s$ peaks near $\phi_s = 0$, as expected for the π exchange Deck graph, the overall distribution is much more symmetric than would be consistent with π exchange only. The need for a substantial contribution from a^* exchange seems demanded. For $Kp \to K^*\pi p$, the K^* exchange graph appears to have weight roughly equal to that of π exchange.

The inclusion of a K^* exchange graph in the Deck model description of $K^o p \to Q^o p$ and $\overline{K^o} p \to \overline{Q^o} p$ may resolve also the erroneous prediction of the cross-over systematics, obtained from the π exchange Deck graph only. This proposal can be tested in detail with the SLAC $K^o_L p$ data, by means of the $\cos\phi_s$ selections described above.

The reactions $\pi^\pm p \to \pi^\pm(\pi^- \Delta^{++})$ are described by a sum of pion and baryon exchange Deck graphs, whose characteristic cross-over systematics differ in sign. This prediction of the Deck model was verified at 16 GeV/c. The success confirms both the utility of the $\cos\phi_s$ selection procedure and the fact that quantum number characteristics of both Deck model graphs are evident in the data.

The $\cos\phi_s$ selection procedure should be generally useful in $2 \to 3$ particle reactions, not only for processes in the diffraction dissociation class.

In neutron dissociation at FNAL and proton dissociation at the ISR, the structure observed in $d\sigma/dt\, dM$ at small t indicates that diffraction dissociation is a peripheral process in impact parameter, whereas elastic diffraction is central. I summarize here the results of a recent detailed investigation[24] of absorptive corrections to the Deck model for diffraction dissociation. We demonstrated that absorption of the expected strength reproduces quantitatively the mass-dependent structure in momentum transfer observed in the Fermilab data[17] on diffractive neutron dissociation $np \to (p\pi^-)p$ and ISR data[16] on proton dissociation $pp \to p(n\pi^+)$. This agreement supports the Deck interpretation of the kinematic nature of diffractive threshold enhancements, and the necessity for absorptive corrections to the model. There are no undetermined parameters in our approach.

In examining $d\sigma/dt\, dM$ at small t, we find that there is a pronounced decrease of the slope in t with increasing M. This mass-slope correlation

is present in the unabsorbed Deck model, but it is considerably accentuated in the absorbed model (Fig. 11). We note also that the mass-slope correlation is a property of the dominant $L = 0$ partial wave in both the absorbed and unabsorbed models. In other words, in our model, a strong decrease of production slope with mass occurs even if only the dominant $L = 0$ wave were present in the data. This contrasts with other approaches[19,25] in which the mass-slope correlation owes its existence to the presumed increase with M of contributions from states of higher L and helicity. The two viewpoints can be tested by partial wave analyses of inelastic diffractive data. Present sketchy results[26] support our viewpoint.

TABLE I

Locations in $|t_1|$ of the zeros in the amplitudes for producing various states of s-channel spin and helicity $[L,\lambda_s]$ are given as a function of mass M of the $(n\pi^+)$ system, from our absorbed Deck model of $pp \to p(n\pi^+)$ at 100 GeV/c. The first column lists values of $[L,\lambda_s]$. Zeros for three different mass values are listed in columns 2-4.

Dip Positions in $(GeV/c)^2$ as a Function of Mass

$L\lambda_s$	$M_{n\pi^+}$ = 1.1 GeV	1.3 GeV	1.5 GeV
00	0.29	0.37	0.43
10	0.33	0.47	0.63
11	0.48	0.67	0.80
20	0.17	0.33	0.45
21	0.63	> 1	> 1
22	0.66	0.93	> 1

REFERENCES

1. H. M. Chan, K. Kajantie, and G. Ranft, Nuovo Cim. 49A, 157 (1967); F. Zachariasen and G. Zweig, Phys. Rev. 160, 1326 (1967); N. Bali, G. F. Chew, and A. Pignotti, Phys. Rev. 163, 1572 (1967).
2. E. L. Berger in Phenomenology in Particle Physics, 1971, Proc. of the Caltech Conference, ed. by C. B. Chiu, G. C. Fox, and A. J. G. Hey.
3. For a review and list of references to earlier work, consult E. L. Berger, "A Critique of the Reggeized Deck Model" Argonne report ANL/HEP 7506, Daresbury Study Weekend Series No. 8, ed. by J. B. Dainton and A. J. G. Hey. E. L. Berger, Phys. Rev. 166, 1525 (1968) and 179, 1567 (1969).
4. L. Montanet and J. Vergeest, TC-Division, CERN, private communication.
5. S. Stergiou, TC Division, CERN, private communication.
6. Aachen-Berlin-CERN-London-Vienna Collaboration, to be published.
7. J. Hanlon, et al., Vanderbilt report VAND-HEP 74(2).
8. I. Ambats, et al., Phys. Rev. D9, 1179 (1974).
9. Aachen-Berlin-Bonn-CERN-Heidelberg Collaboration, J. V. Beaupre, et al., Phys. Letters 41B, 393 (1972).
10. Athens-Bruxelles-CERN-Democritos-Liverpool-Mons-Vienna Collaboration, A. Stergiou, et al., CERN report D.Ph.II/Phys. 74-48, ($K^{\pm}p$ at 8 GeV/c); P. J. Davis, et al., Phys. Rev. D5, 2688 (1972), ($K^{+}p$ at 12 GeV/c); R. Barloutaud, et al., Nucl. Physics B59, 374 (1973), ($K^{-}p$ at 14 GeV/c).
11. G. W. Brandenburg, et al., Nucl. Physics B45, 397 (1972).
12. E. L. Berger, "Systematics of Cross-Over Effects in Inelastic Diffraction Dissociation", Argonne Report ANL/HEP 7464, to be published in Phys. Rev., May or June 1975.

13. Aachen-Berlin-Bonn-CERN-Heidelberg Collaboration, to be published.

14. G. Cohen-Tannoudji, A. Santoro, and M. Souza, Saclay report D.Ph-T 75/41.

15. G. C. Fox and A. J. G. Hey, Nuclear Phys. B56, 386 (1973).

16. CERN-Hamburg-Orsay-Vienna ISR Collaboration. E. Nagy, et al., CERN report submitted to the 17th International Conference on High Energy Physics, London, July, 1974. ($pp \to p(n\pi^+)$ at $\sqrt{s}$ = 23 to 62 (GeV).

17. Northwestern-Rochester-Fermilab Collaboration, J. Biel, et al., reports submitted to the International Conference on High Energy Physics, Palermo, June, 1975 ($np \to pp\pi^-$ from 50 to 300 GeV/c).

18. U. Amaldi Rapporteurs Report, Aix-en-Provence Conference, 1973, Journal de Physique, C1 (1973), p. 241.

19. N. Sakai and J. N. J. White, Nucl. Phys. B59, 511 (1973), and Lett. Nuovo Cimento 8, 618 (1973). M. Jacob and R. Stroynowski, Nucl. Phys. B82, 189 (1974); G. Kane, Acta. Phys. Pol. B3, 845 (1972)

20. R. M. Edelstein, et al., Phys. Rev. D5, 1073 (1972); J. V. Beaupre, et al., Nucl. Phys. B66, 93 (1973); J. Hanlon, et al., Vanderbilt report VAND-HEP 74(2); Scandinavian Bubble Chamber Collaboration, unpublished data on $pp \to pn\pi^+$ at 19 GeV/c, as quoted by G. Kane, ibid.

21. H. Miettinen and P. Pirila, Phys. Letters 40B, 127 (1972).

22. J. D. Jackson, Rev. Mod. Phys. 42, 12 (1970). F. S. Henyey, G. L. Kane, J. Pumplin and M. Ross, Phys. Rev. 182, 1579 (1969).

23. M. L. Good and W. D. Walker, Phys. Rev. 120, 1857 (1960); E. L. Feinberg and I. Pomeranchuk, Suppl. Nuovo Cimento 3, 652 (1956); A. Bialas, W. Czyz, and A. Kotanski, Ann. of Phys. (NY), 73, 439 (1972); J. Pumplin, Phys. Rev. D4, 3482 (1971) and D7, 795 (1973).

24. E. L. Berger and P. Pirila, "Absorptive Effects in Exclusive Diffraction Dissociation" Argonne report ANL-HEP-PR-75-27, June 1975, submitted to Phys. Rev. Different approaches are discussed by V. A. Tsarev, Phys. Rev. D11, 1864 (1975) and G. Cohen-Tannoudji and U. Maor, Saclay report D.Ph-T/75/38 (1975).

25. S. Humble, Nucl. Phys. B76, 137 (1974) and B86, 285 (1975).

26. Yu. M. Antipov, et al., Nucl. Phys. B63, 153 (1973). I am grateful to R. Cutler for calling my attention to Table 1 of this reference.

27. E. L. Berger and G. C. Fox, Proc. IInd International Conference on Polarized Targets, Berkeley, 1971, ed. by G. Shapiro; G. C. Fox, Phys. Rev. D9, 3196 (1974).

FIGURE CAPTIONS

1. (a) Diagram illustrating the independent Lorentz invariant kinematic variables for $ap \to a^* \pi p$.

   (b) Doubly-peripheral exchange graph for $ap \to 123$. Symbols R_1 and R_2 denote exchanges.

2. The two pole terms for the diffractive process $ap \to a^* \pi p$. The wavy line labelled P denotes the full elastic scattering amplitude.

   (a) The "t-channel" pion exchange pole graph;

   (b) the "u-channel" a^* exchange pole graph.

3. Diagram in which the s-channel decay angles (θ_s, ϕ_s) of $A^* \to (a^* \pi)$ are defined, for the reaction $ap \to A^* N$.

4. The distribution $d\sigma/d\phi_s$ for $K^- p \to K^*_{890} \pi N$ as obtained from the π exchange Deck model at 14 GeV/c. The selections Mass $(K^* \pi) \leq 1.5$ GeV and Mass $(N\pi) \geq 1.34$ GeV were imposed. The full distribution is for the "diffractive" reaction (in which N = proton), whereas the shaded distribution is for the charge-exchange process. The normalization is in arbitrary units for both reactions, adjusted so that the cross-sections at $\phi_s = 0$ are equal. Results are presented in histogram form, as obtained from the Monte Carlo event generator. For details of the calculation, see Ref. 3.

5. Pion-exchange Deck graphs for the processes $\pi^\pm p \to \rho^0 \pi^\pm p$ and $K^\pm p \to K^{*0} \pi^\pm p$.

6. Pion-exchange Deck graphs for

   (a) $K^0 p \to K^{*+} \pi^- p$ and

   (b) $\bar{K}^0 p \to K^{*-} \pi^+ p$.

7. The B-ω exchange graphs proposed in Ref. 14.

8. The two-dimensional decay phase-space of $A^* \to a^*\pi$ in terms of the t-channel decay angles. At high energy the π exchange and a^* exchange Deck graphs of Fig. 2 concentrate events into the two corners noted in the figure.

9. Diagram illustrating the kinematic variables for the absorptive graph. All wavy lines denote elastic scattering.

10. Doubly differential cross-section $d\sigma/dt\,dM$ for $pp \to p(n\pi^+)$ at 100 GeV/c and its decomposition into partial cross-sections for individual spin-helicity states of the $(n\pi^+)$ system. The states are labelled by the orbital angular momentum L and s-channel helicity λ_s of the $(n\pi^+)$ system, with the intrinsic spins of the nucleons ignored. For $\lambda_s \neq 0$, curves denote the sum of cross-sections for (L, λ_s) and $(L, -\lambda_s)$. Results for the unabsorbed model are given in part (a); these for the absorbed model in (b). The overall normalization is arbitrary, but the relative normalization of curves within part (a) and with part (b) is fixed by the model. The relative normalization between parts (a) and (b) is also determined by the model.

11. Logarithmic slope of the momentum transfer t_{pp} dependence for nucleon dissociation $Np \to (N\pi)p$ at 100 GeV/c as a function of the mass of the $(N\pi)$ system. Results are shown for (a) the total cross-section $d\sigma/dt\,dM$ and (b) the $(N\pi)$ s-wave component. Data from Ref. 17 on neutron dissociation are listed in (a).

12. Polarizations of the final nucleon in $pp \to p(n\pi^+)$ and $pp \to p(\Delta^{++}\pi^-)$ at 6 GeV/c as a function of momentum transfer t. The unabsorbed pion exchange Deck model predictions are taken from the paper by

Fox, Ref. 27. The values of excitation mass are listed. The absorbed Deck model expectations are discussed in the text of this article.

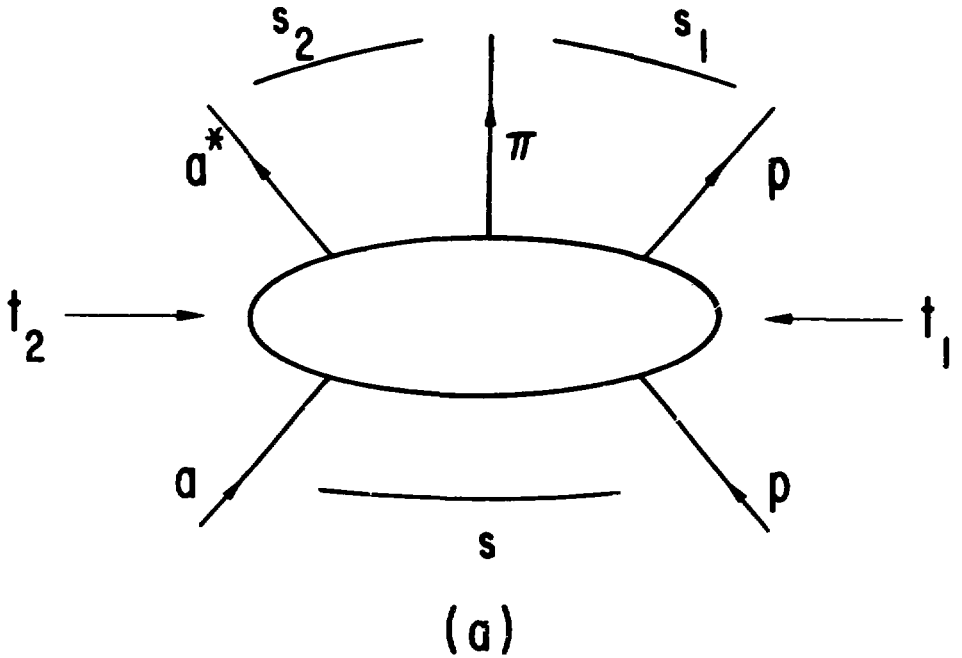

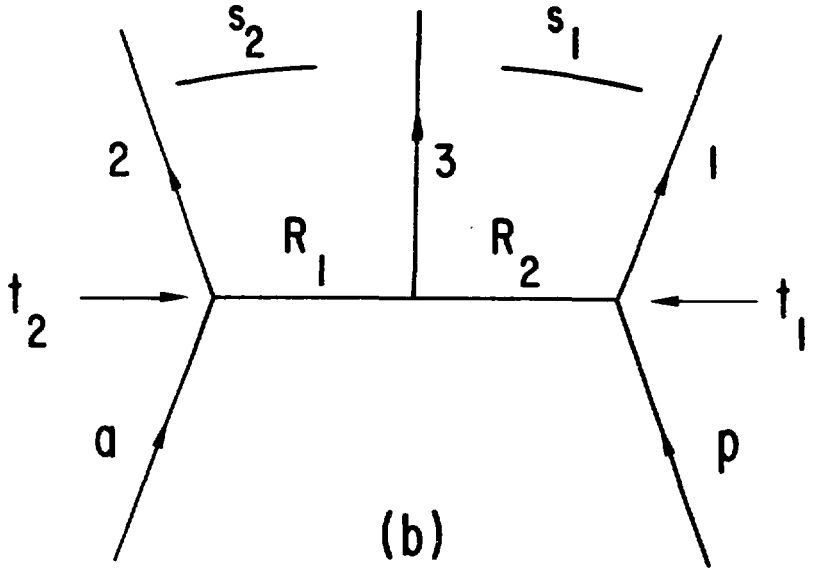

Figure 1

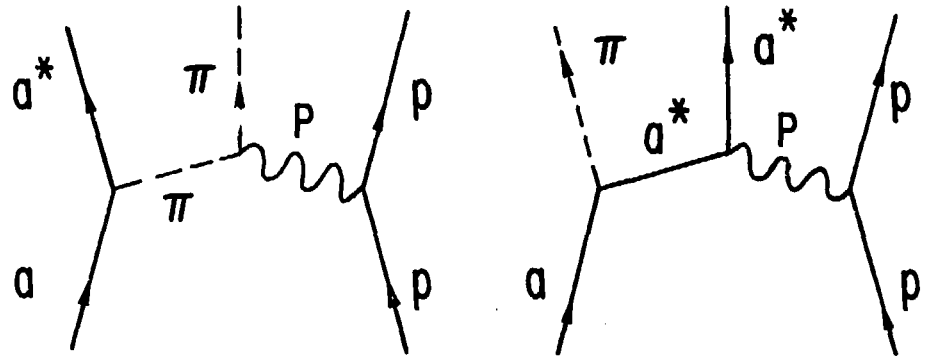

Figure 2

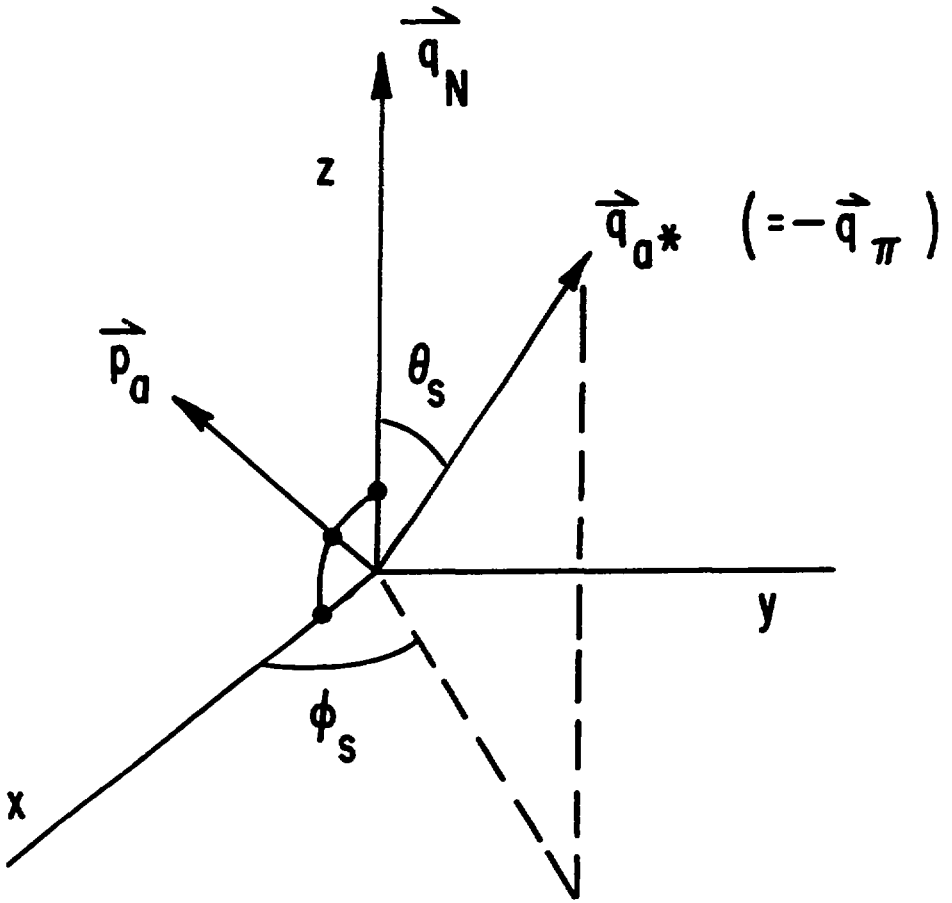

$$a\,p \longrightarrow a^*\,\pi\,N$$

S CHANNEL

Figure 3

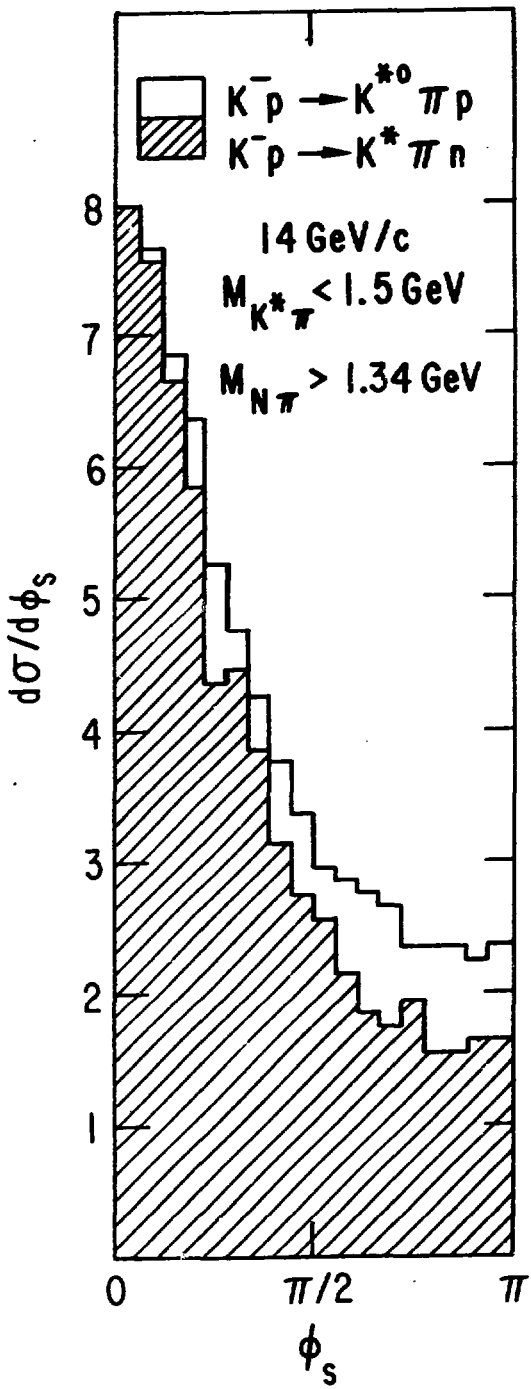
$K^- p \to K^{*0} \pi p$
$K^- p \to K^* \pi n$
14 GeV/c
$M_{K^*\pi} < 1.5$ GeV
$M_{N\pi} > 1.34$ GeV
$d\sigma/d\phi_s$
8
7
6
5
4
3
2
1
0
$\pi/2$
π
ϕ_s

Figure 4

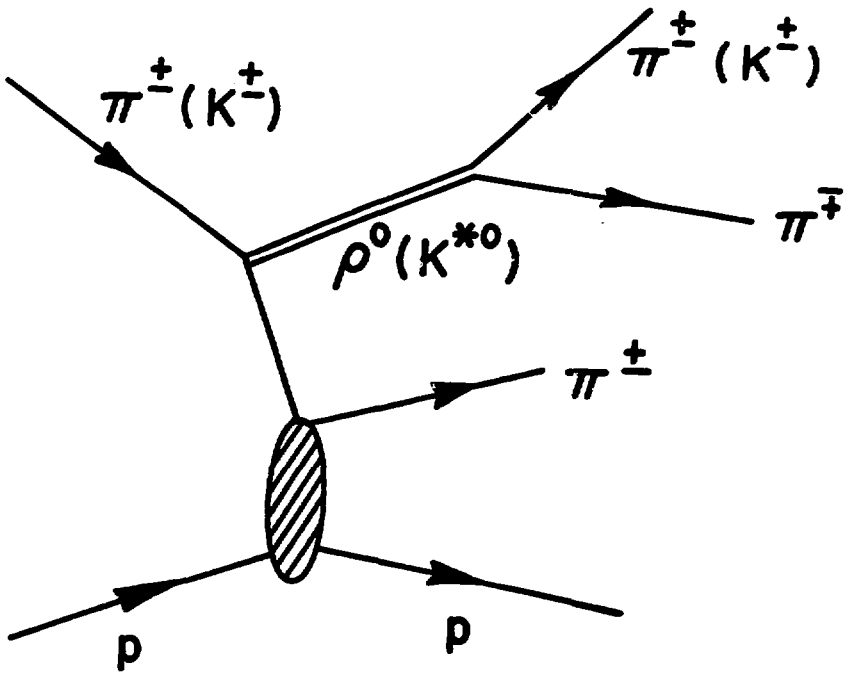

Figure 5

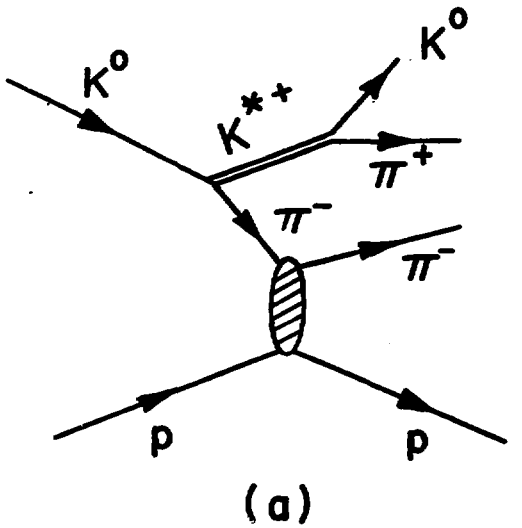

(a)

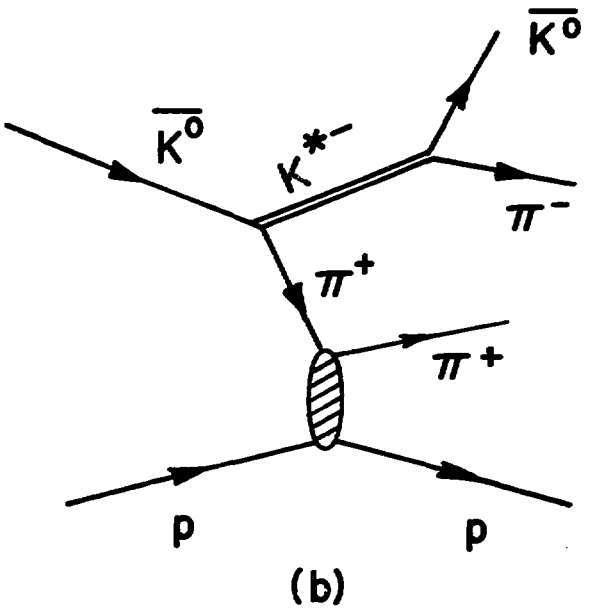

(b)

Figure 6

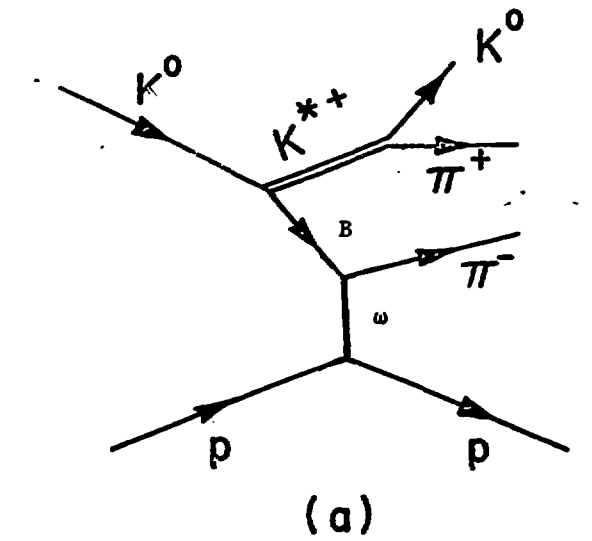

(a)

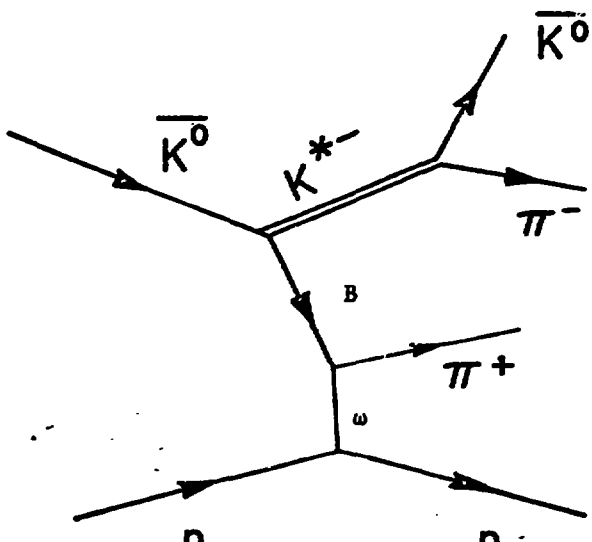

(b)

Figure 7

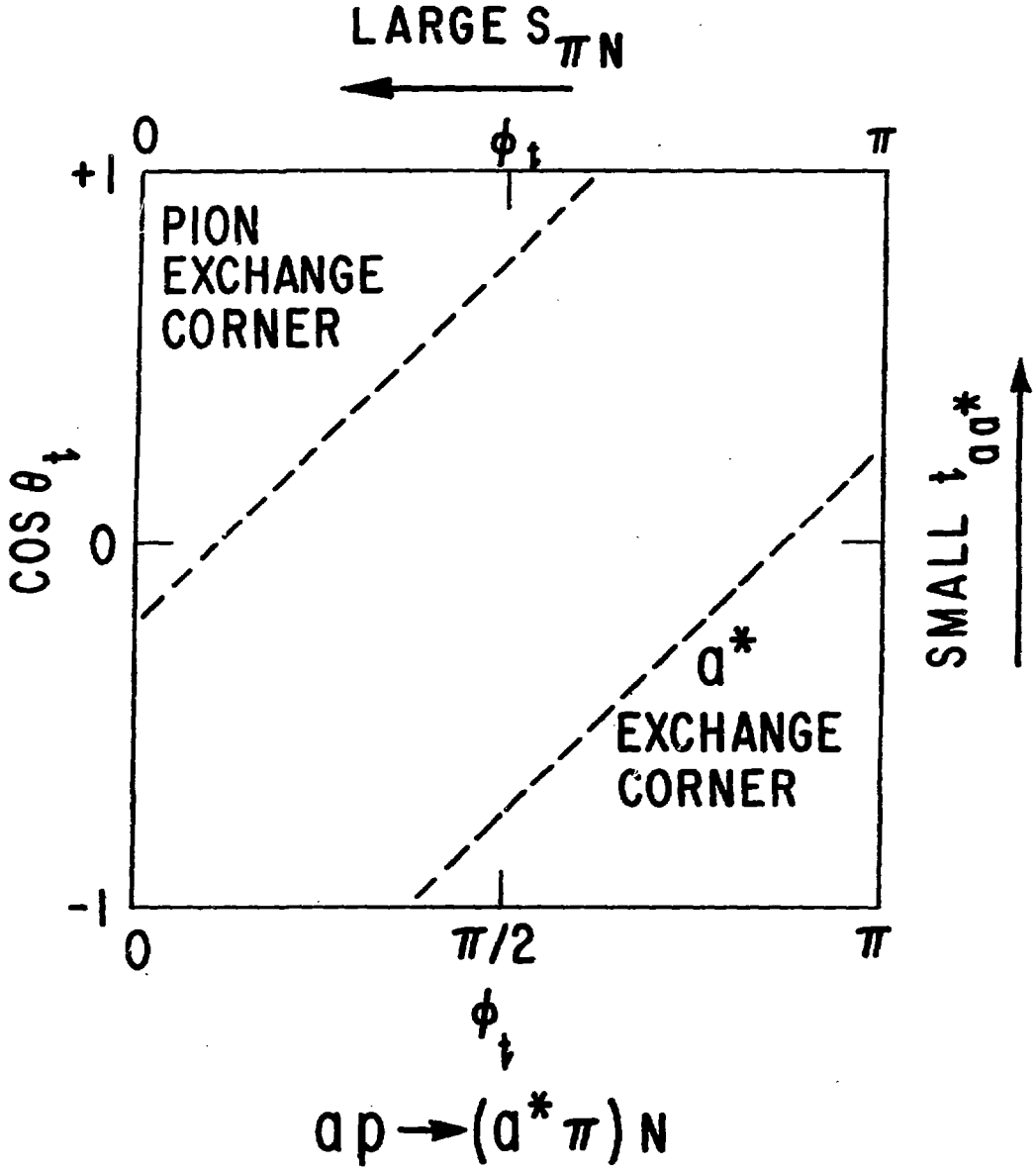
LARGE $S_{\pi N}$
0
ϕ_t
π
+1
PION
EXCHANGE
CORNER
$\cos\theta_t$
0
a^*
EXCHANGE
CORNER
SMALL t_{aa^*}
-1
0
$\pi/2$
π
ϕ_t
$ap \rightarrow (a^*\pi)N$

Figure 8

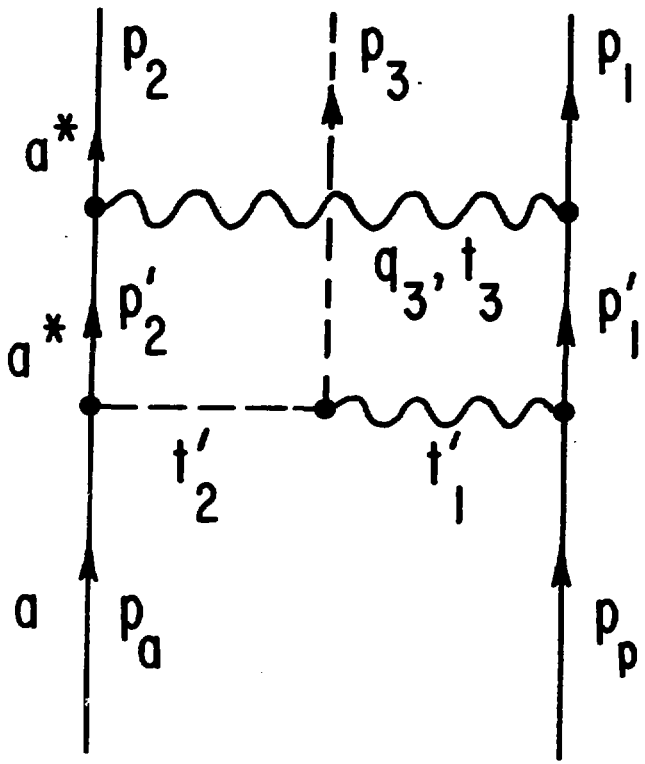

Figure 9

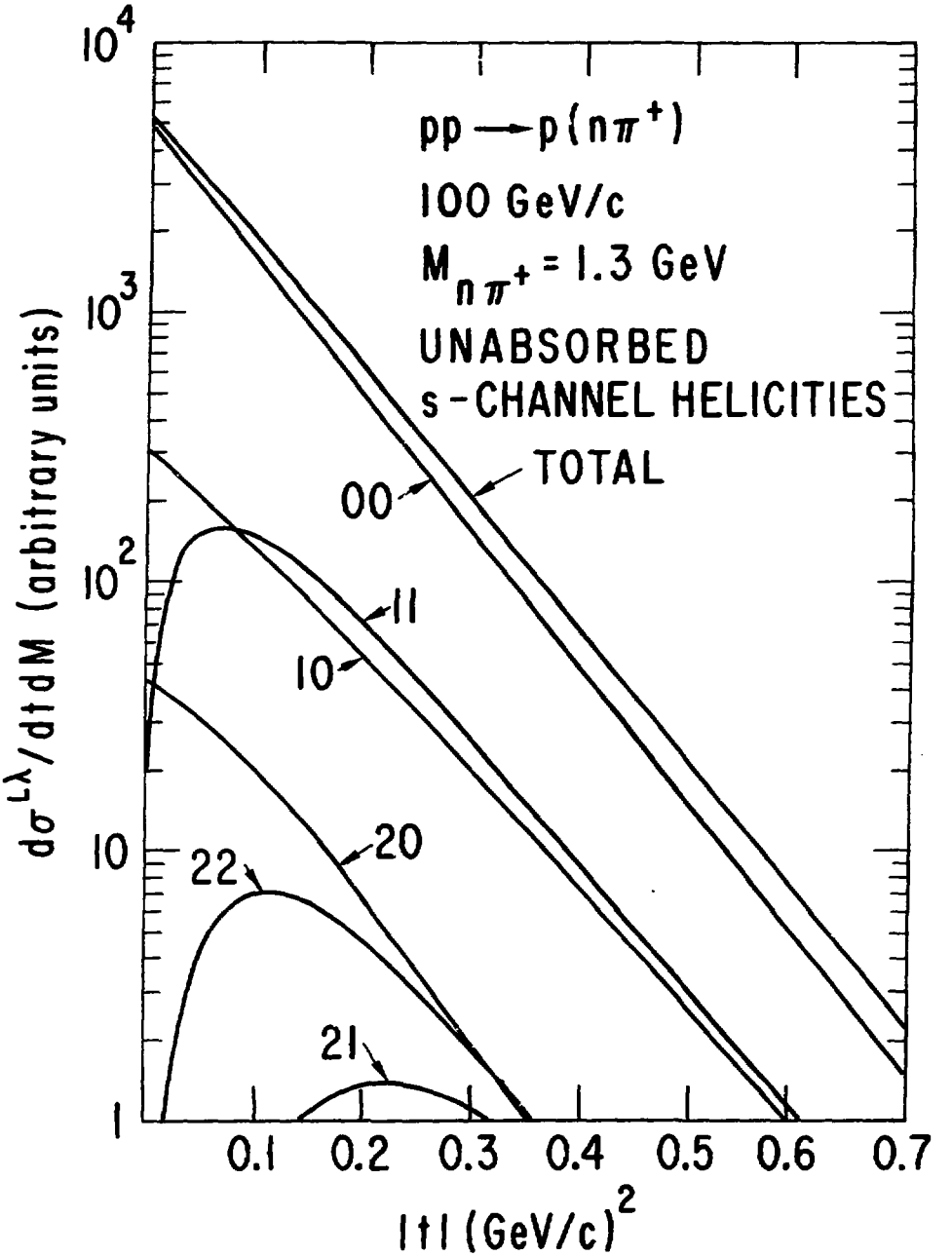
10^4
10^3
10^2
10
1
$d\sigma^{L\lambda}/dtdM$ (arbitrary units)
$pp \rightarrow p(n\pi^+)$
100 GeV/c
$M_{n\pi^+}$ = 1.3 GeV
UNABSORBED
s-CHANNEL HELICITIES
TOTAL
00
11
10
20
22
21
0.1
0.2
0.3
0.4
0.5
0.6
0.7
$|t|$ (GeV/c)^2

Figure 10(a)

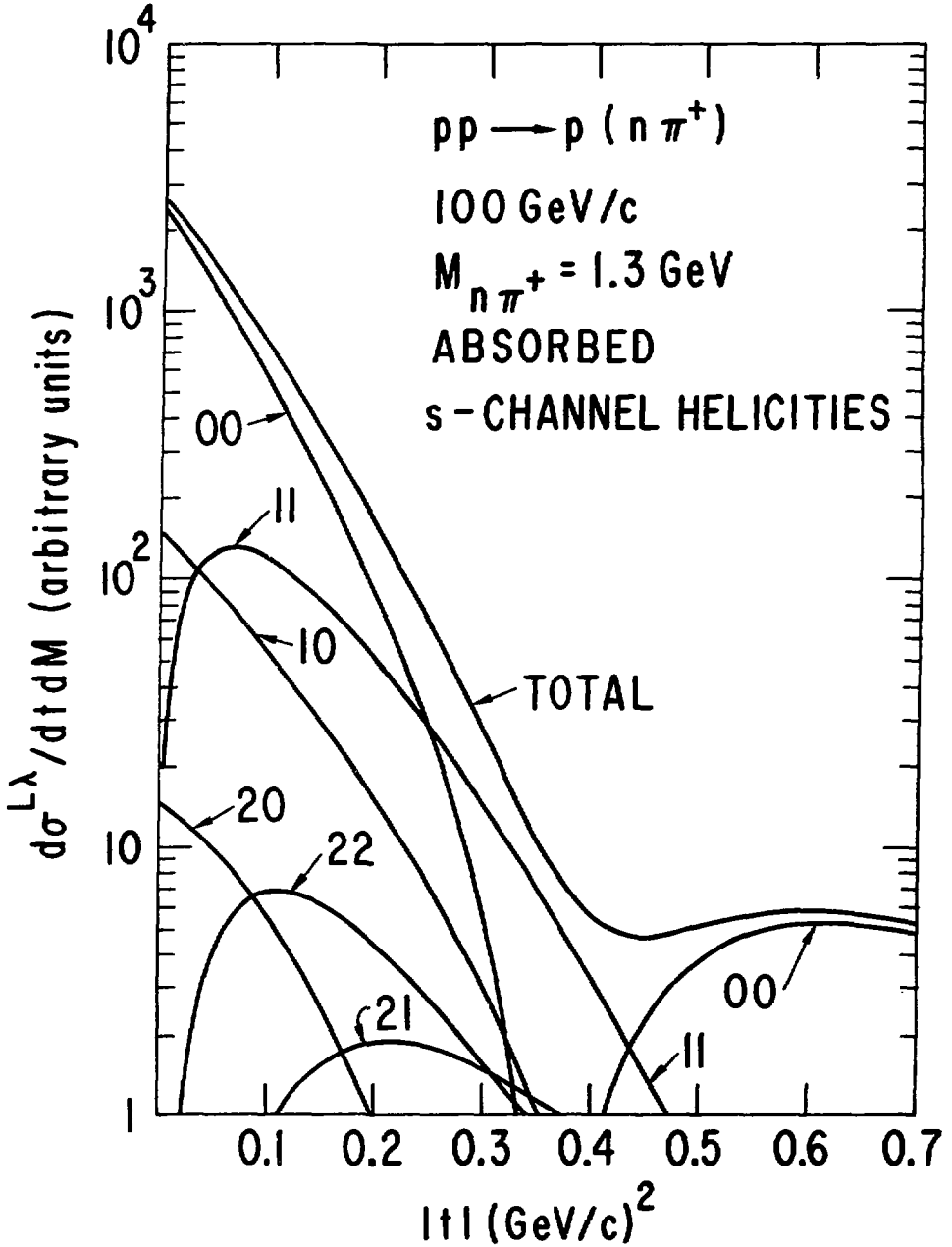
10^4
10^3
10^2
10
1
$pp \longrightarrow p\,(n\pi^+)$
100 GeV/c
$M_{n\pi^+}$ = 1.3 GeV
ABSORBED
s-CHANNEL HELICITIES
00
11
10
TOTAL
20
22
21
00
11
$d\sigma^{L\lambda}/dt\,dM$ (arbitrary units)
0.1
0.2
0.3
0.4
0.5
0.6
0.7
$|t|$ (GeV/c)^2

Figure 10(b)

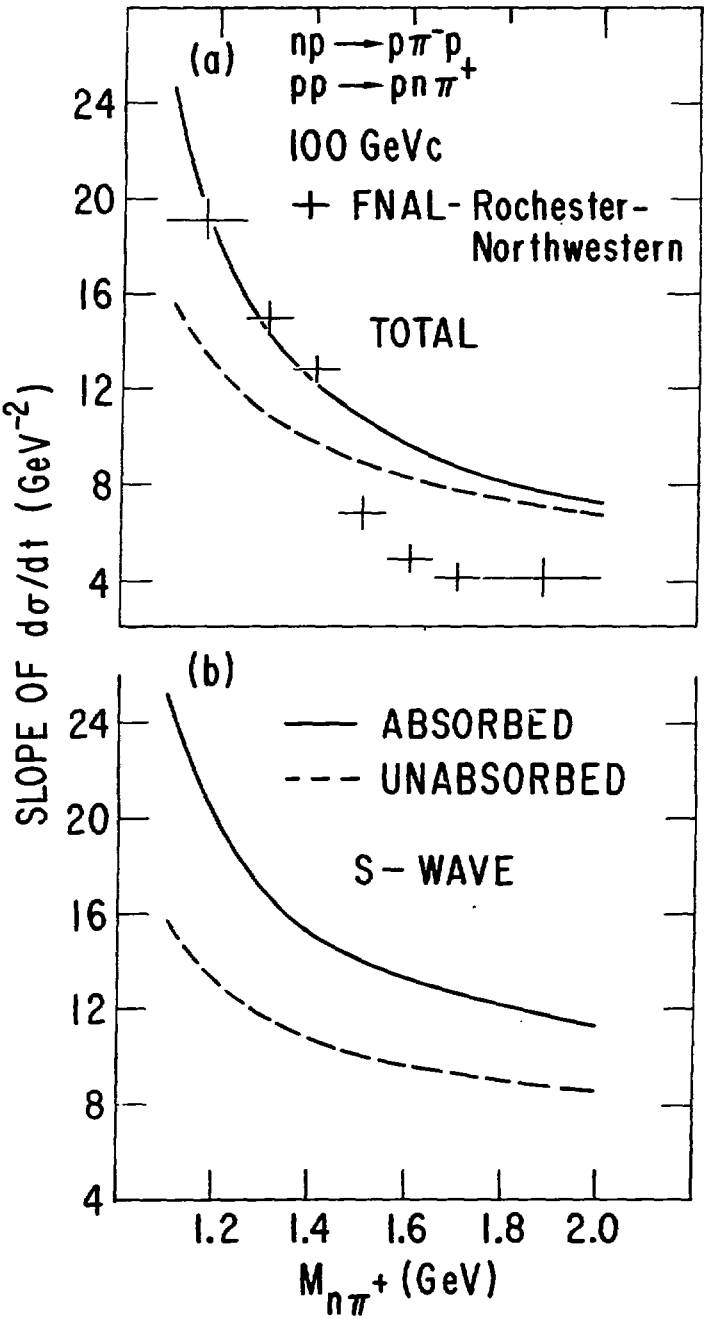
(a)
np → pπ⁻p₊
pp → pnπ⁺
100 GeVc
+ FNAL-Rochester-Northwestern
TOTAL
(b)
ABSORBED
UNABSORBED
S-WAVE
SLOPE OF dσ/dt (GeV⁻²)
24
20
16
12
8
4
1.2
1.4
1.6
1.8
2.0
M nπ+ (GeV)

Figure 11

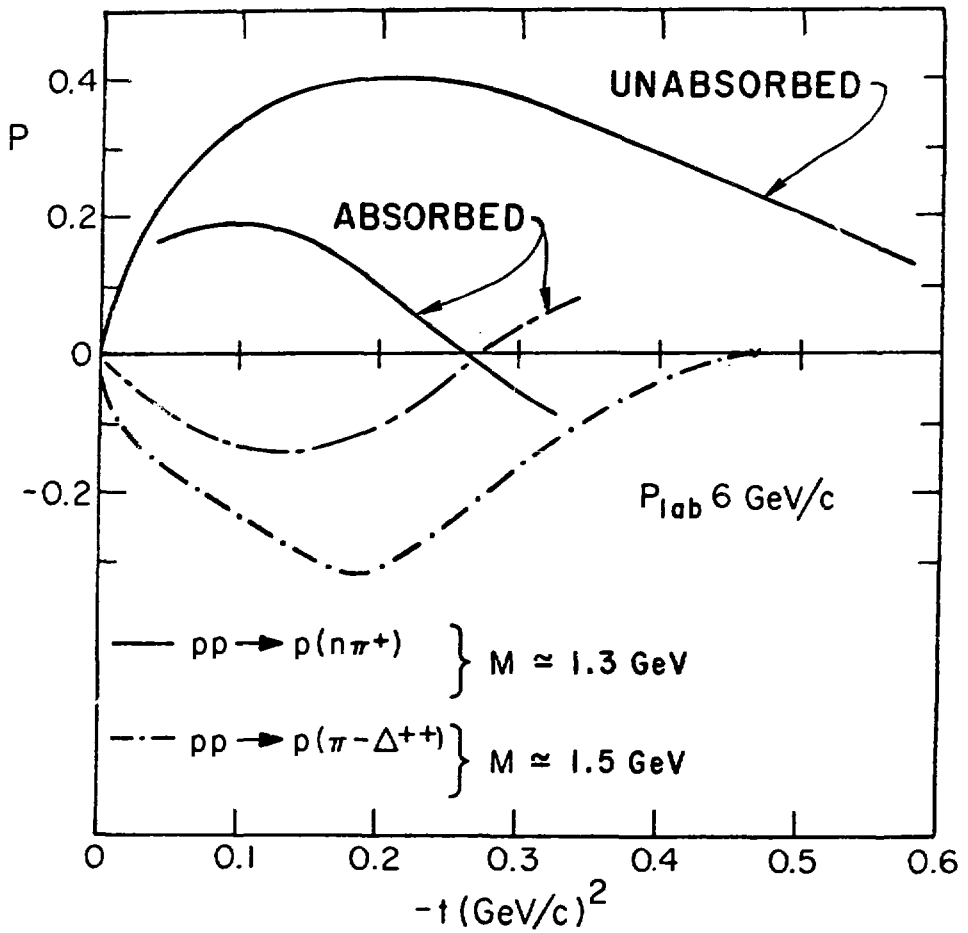
0.4
P
0.2
0
-0.2
UNABSORBED
ABSORBED
P_{lab} 6 GeV/c
pp → p(nπ+)
M ≃ 1.3 GeV
pp → p(π−Δ++)
M ≃ 1.5 GeV
0
0.1
0.2
0.3
0.4
0.5
0.6
$-t\,(GeV/c)^2$

Figure 12

TABLE I

Locations in $|t_1|$ of the zeros in the amplitudes for producing various states of s-channel spin and helicity $[L,\lambda_s]$ are given as a function of mass M of the $(n\pi^+)$ system, from our absorbed Deck model of $pp \to p(n\pi^+)$ at 100 GeV/c. The first colum lists values of $[L,\lambda_s]$. Zeros for three different mass values are listed in columns 2-4.

Dip Positions in $(GeV/c)^2$ as a Function of Mass

$L\lambda_s$	$M_{n\pi^+}$ = 1.1 GeV	1.3 GeV	1.5 GeV
00	0.29	0.37	0.43
10	0.33	0.47	0.63
11	0.48	0.67	0.80
20	0.17	0.33	0.45
21	0.63	> 1	> 1
22	0.66	0.93	> 1

TABLE I

Locations in $|t_1|$ of the zeros in the amplitudes for producing various states of s-channel spin and helicity $[L,\lambda_s]$ are given as a function of mass M of the $(n\pi^+)$ system, from our absorbed Deck model of $pp \to p(n\pi^+)$ at 100 GeV/c. The first column lists values of $[L,\lambda_s]$. Zeros for three different mass values are listed in columns 2-4.

Dip Positions in $(GeV/c)^2$ as a Function of Mass

$L\lambda_s$	$M_{n\pi^+}$ = 1.1 GeV	1.3 GeV	1.5 GeV
00	0.29	0.37	0.43
10	0.33	0.47	0.63
11	0.48	0.67	0.80
20	0.17	0.33	0.45
21	0.63	> 1	> 1
22	0.66	0.93	> 1